IEEE Access
Multidisciplinary | Rapid Review | Open Access Journal

Received March 23, 2018, accepted May 4, 2018, date of publication May 15, 2018, date of current version June 5, 2018.

Digital Object Identifier 10.1109/ACCESS.2018.2834906

Power System Transient Stability: An Algorithm for Assessment and Enhancement Based on Catastrophe Theory and FACTS Devices

MAI MAHMOUD ELADANY, AZZA AHMED ELDESOUKY, AND ABDELHAY AHMED SALLAM, (Life Senior Member, IEEE)
Electrical Power Department, Port Said University, Port Fouad 42526, Egypt
Corresponding author: MAI M. ELADANY (mai_eladany@eng.psu.eg)

ABSTRACT It is of crucial importance to obviate power system damage and cascading failures that may cause a full or partial blackout when the system is exposed to severe contingencies. Flexible alternating current transmission system (FACTS) devices have been harnessed for solving several power system problems including transient stability. Ever since, to emphasize the effectiveness of the FACTS technology, the number and allocation of these devices must be selected properly. So, a novel algorithm is proposed in this paper to determine the best least number (BLN) and allocation of the thyristor-controlled series capacitor (TCSC) with a goal of improving the transient stability in an optimal manner. A combination of the catastrophe theory (CT) and the multi-objective particle swarm optimization (MOPSO) method in addition to a clustering technique is used to structure the proposed algorithm. The CT is used to assess the transient stability and calculate the critical clearing time (CCT). MOPSO is applied to compromise between maximizing the CCT and minimizing the cost of TCSCs as two contradictory objective functions. The clustering technique is designed to provide the BLN of TCSC devices. Accordingly, at least investment, the proposed algorithm satisfies an increase of the stability margin by increasing the value of CCT for each generator and improves the location of operating points in the CT's stability region. Simulation of the proposed algorithm application to New England 39-bus power system is presented to verify the algorithm effectiveness. The results confirm the feasibility of this algorithm and are validated in comparison with those obtained through time-domain simulation.

INDEX TERMS Catastrophe theory, FACTS devices, multi-objective particle swarm optimization, transient stability.

I. INTRODUCTION

Transient stability analysis is essential for evaluating the network's ability to regain an adequate state of equilibrium after being prone to either large or small disturbances [1]. Therefore, use of accurate methods to assess the transient stability is vital in preventing such conditions and hence of special interest in the field of power system security. Critical clearing time (CCT), which is defined as'' maximal fault duration for which the system remains transiently stable,'' is an important parameter to specify the transient stability state of power systems [2]. Several research works have dealt with calculating CCT in multi-machine power system either by direct methods based on transient energy function (TEF) or step-by-step time domain simulation (TDS) methods or artificial intelligence techniques [3]–[6]. CCT is also calculated in [7] as a linear function in terms of the generator rotor angle at the faulted bus.

Calculation of CCT, precisely and directly, without any assumptions or using trial and error approximated methods could be done by using catastrophe theory (CT), which is fast and direct assessment method. CT is featured as a qualitative and effective mathematical tool for studying both transient and steady-state stability of power systems [8], [9]. It is initially presented in [10] to study power system steady state stability, and then, compared with the energy balance approach. The results approved that the cusp manifold can be used to assess the power system steady state stability [11]. CT has also been applied to transient stability assessment of multi-machine power system by defining the stability region in the cusp bifurcation surface in terms of defined control variables [12]. In addition, CT has been studied to provide the swallowtail manifold by which the multi-machine power system transient stability can be assessed online [13].

It is beneficial to enhance the power system transient stability with a goal of enabling the system to withstand more severe contingencies (i.e., to be more secure). Stability enhancement can be achieved by designing effective controllers and adding compensating devices in an optimal manner. Different optimization techniques have been employed for this purpose [14]. Multi-objective particle swarm optimization (MOPSO) method has shown the competence to untangle multi-objective problems in many fields [15]. MOPSO is used in [16] in order to find Pareto set of corrected transient energy margin and congestion management cost as two conflicting objective functions. Due to MOPSO outstanding performance in solving nonlinear objectives, it is used in [17] to improve the dynamic stability of multi-source power system. It is also considered as an effective method to find the optimal allocation of static VAR compensators (SVCs) in a multi-machine power system to enhance the transient stability [18].

Flexible alternating current transmission system (FACTS) devices can be used to improve power system dynamics, e.g., transient stability, oscillations dampening, voltage control, voltage stability and reliability [19]. It has evolved in two generations; the first generation comprises (SVC) and the thyristor-controlled series capacitor (TCSC). The second generation encompasses static synchronous compensator (STATCOM), the static synchronous series compensator (SSSC), and the unified power flow controller (UPFC). Specifically, FACTS devices for series compensation provide the system with reactive power that increases the natural power of the transmission line, which in turn, increases its power transfer capacity. This results in an enhancement of the system transient stability [20]. SSSC, which is classified as a voltage source converter-based FACTS controller is capable of interchanging active and reactive power with the power system [21], [22]. Nonetheless, the transformer needed to connect SSSC in series with the transmission line is a cost disadvantage and reduces the performance of the SSSC due to an extra reactance being introduced. Also, the source of energy, which is needed to provide the DC voltage across the capacitor and make up for the losses of the voltage source converter (VSC) could cause compensation limitation on the required device [20]. TCSC can be considered as one of the effective and economic FACTS controllers. It is progressively employed in stressed and congested transmission systems [23]. The effectiveness depends mainly on their sizes and places in the power system [24].

Particularly, for transient stability enhancement, TCSC proved its superiority and can outweigh the other FACTS devices because the TCSC controls the line reactance directly not through injecting voltage into the line [25]–[27]. Many studies have demonstrated the role of TCSC for enhancing power system performance and still are in action so far [28]–[31]. Adaptive differential evolution algorithm is used in [32] in order to find the efficient allocation of TCSC devices. In addition, a proposed multi-objective function has been applied to find a middle ground between reducing power losses, improving voltage profile, reducing reactive power losses, reducing TCSC cost and reducing the number of FACTS units. A local fuzzy based damping controller for TCSC is investigated in [33]. In order to control TCSC firing angle, the frequency at the TCSC bus is used as a local feedback signal and the chaotic optimization algorithm, as a heuristic algorithm, is used to adjust the parameters of the controller. A new nonlinear control scheme for TCSCs has been suggested to study the transient stability of a multi-machine power system in [34]. Here, zero dynamic design method is used to express the nonlinear control strategy of the TCSC controller. Pre-selected parameters of TCSC and SVC are optimized by using multi-objective self-adaptive evolutionary programming algorithm to enhance the transient stability in [35].

From the literature review, power system transient stability must be assessed as accurate as possible to decide how to improve it. Then, selecting the method being applied to achieve the desired improvement. These methods are either adding some assets into the system (e.g., FACTS devices) or optimizing the performance of the existing system assets (e.g., local controllers of generators and loads) or combination of both.

In this paper, TCSC as one of the FACTS devices is used because of its technical and economic advantages that outweigh those of other devices. A new algorithm is proposed to find the optimal allocation and the best least number (BLN) of TCSC to achieve minimum investment required to improve and maintain system stability. A combination of CT and MOPSO in addition to a clustering technique are the main tools to structure the proposed algorithm. So, the algorithm is based on: *i*- CT for transient stability assessment, *ii*- MOPSO technique for stability improvement by maximizing the CCT and minimizing the cost of TCSC devices as two contradictory objective functions, and *iii*- the clustering technique that is designed to calculate the BLN of the TCSCs from which the devices satisfying the best highest value (BHV) of CCT for each generator is determined.

The next sections are organized as: Section II presents transient stability assessment by using CT. Section III provides a brief review of FACTS devices, particularly, TCSC. The optimal allocation of TCSCs as a multi-objective optimization problem is presented in Section IV. Description of the new algorithm is given in Section V. The applicability of the proposed algorithm is explained in Section VI for all possible line outages and line congestion through an illustrative example that is validated by comparing the results with those obtained by TDS. Section VII summarizes the finding of this work and draws conclusions. Section VIII contains the references. Finally, an Appendix to illustrate some details toward CT.

II. TRANSIENT STABILITY ASSESSMENT BY USING CT

It is found that CT has the capability of representing the operating points of the system's machines within a manifold that defines the stability margin. The location of these operating points is determined by calculating control parameters

(a, b, and c) defined by algebraic equations that yield fast transient stability assessment [11]. For the swallowtail bifurcation catastrophe, the values of the three control variables are computed in terms of the system parameters at different operating conditions. Thus, the corresponding operating points in the control space and their location with respect to the stability boundaries can be defined. The bifurcation set is valid for the power system encountering any type of stresses and congestion. Additionally, CT can visualize the operating points for online monitoring. It has been applied to power system transient stability assessment by deriving the swallowtail bifurcation catastrophe function that is given by [36]

$$y^4 + ay^2 + by + c = o \tag{1}$$

where, y is the state variable calculated in terms of the CCT, and the control variables a, b, and c, which are algebraically expressed in terms of system parameters, i.e., no need to solve the swing equations. It is to be noted that $a = -12$ (i.e., constant) in this application, and so, the swallowtail bifurcation set representing the control space is only dependent on b and c [13]. The derivation is given in Appendix and the graphs of three and two-dimension bifurcation set are shown in Figs. 1a and 1b, respectively. For stable operation of the power system, the operating points of all generators must be inside the shaded area of the graph shown in Fig. 1b.

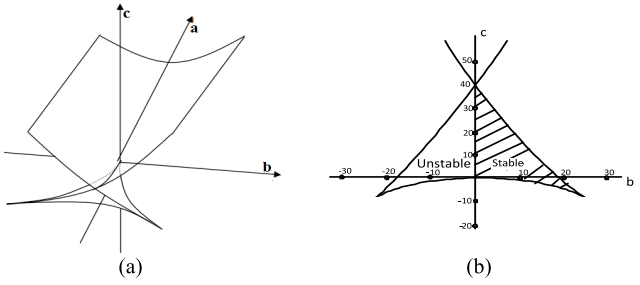

FIGURE 1. Schematic outline of swallowtail bifurcation set. (a) in three-dimension space, (b) in two-dimension space (the shaded area represents the stable region).

III. FACTS DEVICES

FACTS devices can be connected in shunt, in series, or in combination of both. The advantages they offer to the power system are widely referenced in several scientific works. These benefits involve enhancement of power system stability, controlling the flow of active and reactive power in the system, and increasing system loadability [37]. Optimal allocation of FACTS devices enables the existing power systems to be utilized more effectively. TCSC is a type of series compensation that is of interest for several reasons such as [38]

1- providing a way of varying series compensation to instantly meet the system requirements, thereby permitting control of power flow in the compensated transmission line;
2- providing a fast and continuous control scheme that might be used for adding damping to spontaneous system oscillations; and
3- enhancing transient stability, reducing network losses, providing voltage support, limiting short-circuit currents, and mitigating subsynchronous resonance.

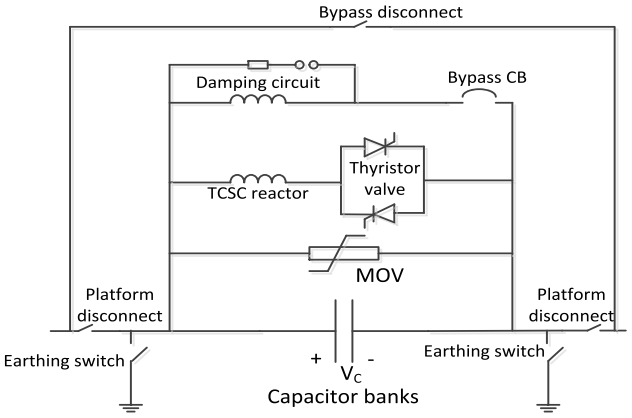

FIGURE 2. The basic structure of TCSC [20].

TCSC can operate in different modes: blocking mode, bypass mode and capacitive boost mode [20]. A typical TCSC module entails a fixed series capacitor, C, in parallel with a thyristor controlled reactor as shown in Fig. 2. This combination allows smooth control of the fundamental frequency capacitive reactance over a wide range. A bypass disconnect switch is used to protect the device in the event of a high fault current on the line. A metal-oxide varistor (MOV) is also connected across the capacitor to prevent over-voltages. TCSC device is connected in series with the transmission line and used to control the real power flow by controlling the electrical length of the transmission line. During the power flow analysis, the TCSC is modeled as a constant capacitive reactance that modifies the line reactance X_L, to become X'_L as in the relation below.

$$X'_L = (1 - \mathcal{K})\, X_{Line} \tag{2}$$

where $\mathcal{K} \triangleq$ the degree of compensation $\left(X_C / X_{Line}\right)$.

IV. TCSC ALLOCATION OPTIMIZATION PROBLEM

PSO technique is one of the most effective metaheuristics algorithms with many successful real-world applications [39]. Considering the cost of TCSC, MOPSO is used in this study to determine the optimal allocation of the TCSC required to maintain system stability when a fault occurs at a predefined location. The fitness function of MOPSO method, F, is formulated in terms of two contradictory objective functions (F_1 represents the value of CCT to be maximized and F_2 to calculate the TCSC cost to be minimized) as given below.

i) The Objective Function F_1: Based on CT, it computes the value of CCT as derived in Appendix and given by (A.37).

Thus, F_1 can be written as [13]

$$F_1 = \left[\sqrt{\frac{2M\,(\delta_c - \delta_0)}{(P_{in} - P_e\,(t_{0+}))}} \right] \tag{3}$$

ii) The Objective Function F_2: It gives the cost of TCSC, (C_{TCSC}). This function can be written in the form [36]

$$F_2 = (0.0015\,S^2 - 0.7130\,S + 153.75) \tag{4}$$

From (3) and (4), the *Fitness Function (F)* can be expressed by using weighted sum method as

$$max\ F = (h_1 F_1 - h_2 F_2) \tag{5}$$

Subjected to *Equality constraints*:

δ_c = the smallest positive real root of (1).

$$S = |Q_2| - |Q_1| \tag{6}$$

Inequality constraints:

$$0 < b < b_{max} \tag{7}$$

$$c_{min} < c < c_{max} \tag{8}$$

$$80\%(capacitive) < k < 20\%(reactive) \tag{9}$$

where,
$\delta_c \triangleq$ critical clearing angle.
$\delta_o \triangleq$ minimum angle of oscillation.
$P_{in} \triangleq$ input mechanical power.
$P_e\,(t_{o+}) \triangleq$ electrical power at the instant of fault.
$M \triangleq$ machine inertia constant.
b and $c \triangleq$ the control parameters, which are the coordinates of generator operating point in the bifurcation set [13]. They are a function of the power delivered by the generator during and after the fault as derived in Appendix and can be calculated by (A.32) and (A.33).
(b_{max}, c_{max}), $(0, c_{min}) \triangleq$ coordinates of the points located on the boundary of the stable region.
$S \triangleq$ the operating range of FACTS devices in MVAR
h_1 and $h_2 \triangleq$ the weighting factor of F_1 and F_2, respectively
Q_1 and $Q_2 \triangleq$ the reactive power flow in the line before and after installation of FACTS device, respectively.

In order to satisfy the system stability, the coordinates of the operating point (b, c) in (1) should not violate the boundary of stability region that is defined in (7) and (8). The degree of TCSC compensation, $\mathcal{K}$, should be within predefined limits as given in (9). The negative sign in (5) denotes the contradiction between F_1 and F_2. Multi-objective optimization based Pareto front methods frequently result in large non-dominated sets, which need significant computation time to be generated, though most of the consistent solutions are irrelevant to the decision maker [40]. Despite the skepticism about its accuracy, weighted sum method offers the opportunity to the decision maker to give the higher weight value to the objective, which he considers as the highest priority [32]. The values of weighting factors could be assigned with different methods such as; analytic network process [41], best worst method [42], aggregated indices randomization method, analytic hierarchy process [43] and choosing by advantages according to the importance of the associated objective function.

V. DESCRIPTION OF THE PROPOSED ALGORITHM

The proposed algorithm applies a combination of CT, and an optimization technique such as PSO to inform decisions about TCSC devices for improving power system stability and maximizing the value of CCT. While the utility has been to plan the allocation of TCSCs first, and then to plan the entailed number of TCSCs, in co-optimization both are assessed to identify a solution that can at least investment cope with all possible contingencies and avoid over-compensation. The three-phase fault, as the most severe fault, as well as the system congestion due to a sudden load increase, are considered to enable the algorithm to deal with the most probable operating conditions. Therefore, the proposed algorithm is divided into two parts (A and B). Algorithm-A is the primary part that is used to determine the optimal allocation of the TCSCs needed to maintain the system stability and maximize the CCT for each fault occurrence at a predefined probable location. The results obtained from algorithm-A are considered as the data being processed by algorithm-B. As an essential complementary part, algorithm 'B' is applied to provide, ***first***, the BLN of TCSCs that satisfies system stability. This can be achieved by a proposed clustering technique. Each TCSC is defined by a set of two elements; location and size. Then, the sets having the same location are grouped together constituting one cluster. An equivalent set for each cluster is determined by two elements (location and the maximum size of the sets included) to specify what is called "cluster-TCSC." The clusters produced are organized in a descending order based on the number of sets included in each cluster. The cluster-TCSCs are inserted frequently (one-by-one) until satisfying the system stability. Accordingly, the BLN of TCSCs can be determined. ***Second***, CT is applied to select which TCSCs can satisfy both system stability and BHV of CCT. So, algorithm-B encompasses two successive sub-algorithms (B1 and B2). The steps of each algorithm are given below and the corresponding flowcharts are shown in Figs. 3, 4, and 5, respectively. As an illustrative example, a test system is studied in the next section for more explanation about the application of the proposed algorithm.

The Steps of primary algorithm-A and complementary algorithm-B

Algorithm-A. Optimal Allocation of TCSCs

1- Initialize the parameters of PSO (number of particles and maximum iteration).
2- Locate the fault on the first line as an initial contingency.
3- Generate initial population randomly.
4- Initialize the location of TCSC.
5- Compute the fitness function.
6- Check stability by CT, if the system is unstable update the position and velocity of particles and go to step 5.

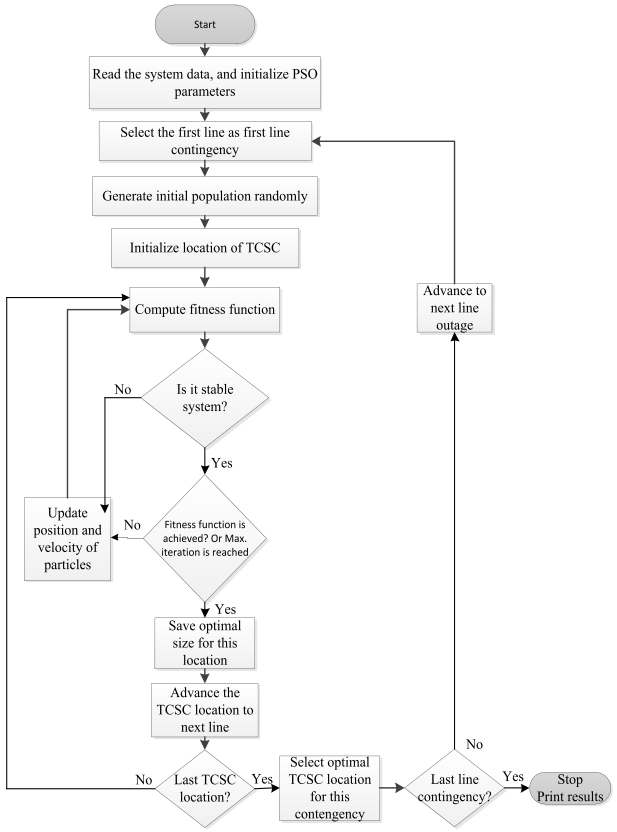

FIGURE 3. Flowchart of Algorithm-A.

7- Check whether the maximum of either iteration number or fitness function is achieved. If yes, then obtain the optimum rating of TCSC for this location.
8- Advance the TCSC location to next line and go to step 5.
9- If all lines are checked for TCSC's location, select the optimal location and size of TCSC for this fault.
10- Consider another line outage and go to step 3.
11- If all faulted lines are checked, stop the process and create a table that gives for each contingency the corresponding optimal allocation of the TCSC.

Algorithm-B. Determination of BLN and BHV

Sub-algorithm-B1. Determination of BLN

Based on the optimal allocation of the TCSCs, obtained from algorithm-A, for probable locations of the three-phase short circuit or sudden load increase, each TCSC is defined by a set of two elements, D_i, that is deduced by

$$D_{\mathrm{i}} = (\ell_i, w_i), \quad i = 1, \ldots N \tag{10}$$

where $N \triangleq$ the number of faulted lines, ℓ_i and W_i are the corresponding location and size of the TCSC, respectively.

1- Clustering these sets into a number of clusters; each cluster 'G' has the sets that are having the same location. The number of sets per cluster is referred to as the location frequency, k, and the clusters are organized in a descending order of k, for example,

$$G_1 \triangleq \left\{(\ell_1, w_{1,1}) \cup (\ell_1, w_{2,1}), \ldots .., \cup (\ell_1, w_{k_1,1})\right\} \tag{11}$$

$$G_2 \triangleq \left\{(\ell_2, w_{1,2}) \cup (\ell_2, w_{2,2}), \ldots .., \cup (\ell_2, w_{k_2,2})\right\} \tag{12}$$

where $k_1 > k_2$

The general form of the jth cluster with location frequency of k_j can be written as

$$G_j \triangleq \left\{(\ell_j, w_{1,j}) \cup (\ell_j, w_{2,j}) .., \cup (\ell_j, w_{k_j,j})\right\}, \quad j = 1, ., M \tag{13}$$

where M$\triangleq$ the number of clusters.

2- Each cluster is represented by what is called 'cluster-TCSC' that is defined by an equivalent set of two elements, $G_{eq,j}$. This set includes the corresponding location and the largest value of the TCSC size encountered in the cluster sets. Thus, from Equation 13, the relation below can be written.

$$G_{eq,j} \triangleq (\ell_j, w_{max,j}), \quad j = 1, \ldots, M \tag{14}$$

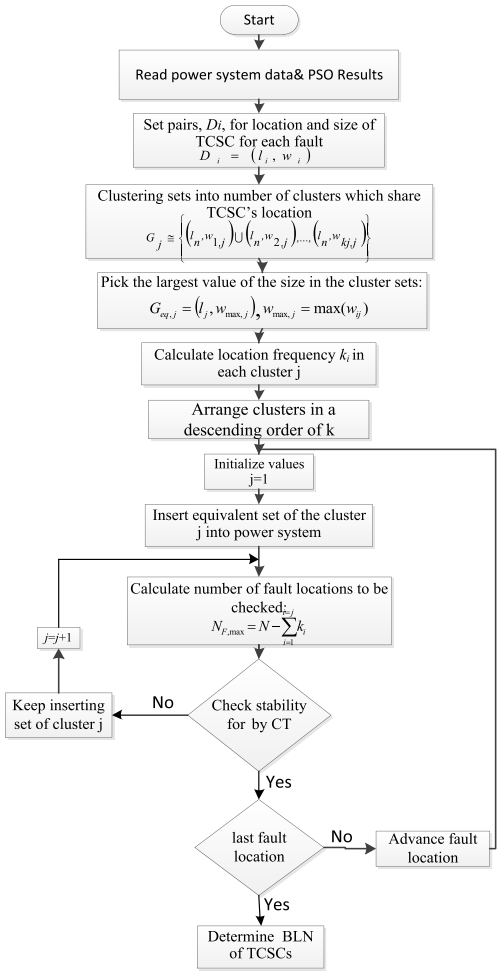

FIGURE 4. Flowchart of sub-algorithm-B1.

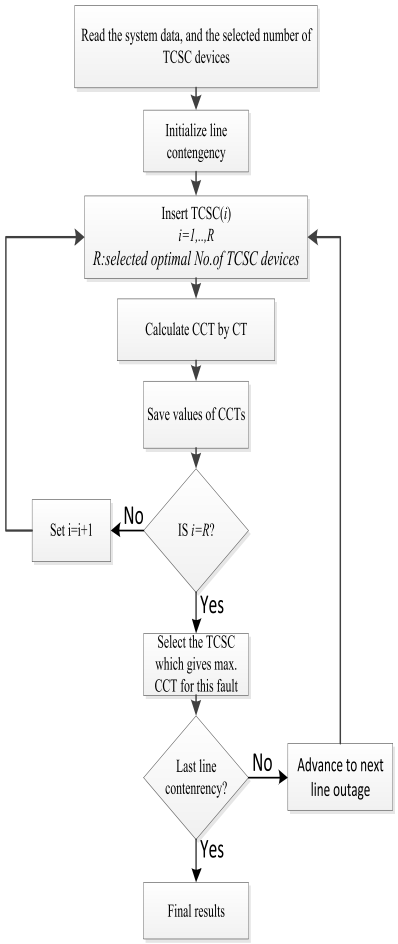

FIGURE 5. Flowchart of sub-algorithm-B2.

where, $w_{max,j} = \max |w_{i,j}|$, $i = 1, ..., k_j$ (with negative and positive sign for capacitive and inductive compensation, respectively)

3- Starting with embedding the cluster-TCSC of the first one (i.e., $j = 1$), as defined by (14), into the power system, CT is applied to assess the system stability for all fault locations excluding those incorporated to this cluster, that is, for a number of fault locations $N_F = N–k_1$.
4- If the system is stable the algorithm will terminate. If not, the cluster-TCSC of the of the next one (i.e. $j = 2$) is additionally embedded into the power system and the system stability is assessed by using CT for the rest number of fault locations that equal $N–k_1–k_2$.
5- Repeating step # 4 to embed the cluster-TCSCs of the next clusters, one-by-one, until the system becomes stable. This can be emphasized by testing the system stability when embedding the j^{th} cluster for a number of fault locations given in a general form as

$$N_F = N - \sum_{i=1}^{i=j} k_i \tag{15}$$

6- Determining the BLN and allocation of TCSC devices required to retain system's stability when contingencies occur (any probable fault or sudden increase of load).

Sub-algorithm-B2. Determination of TCSCs satisfying the BHV of CCT:

1- Starting from the determined allocation of TCSCs set obtained from sub-algorithm-B1 and system data as inputs.
2- At each contingency, CT is used to determine which TCSC device can satisfy BHV of CCT for each generator and enhance the location of operating points by increasing the stability margin in the bifurcation set.

VI. TEST SYSTEM AND RESULTS

The proposed algorithm is applied to 39-bus, ten machines, New England test system as shown in Fig. 6. System data can be found in [44]. MATLAB programming codes are developed for MOPSO where the weighting factors, h_1 and h_2, are assigned by using analytic hierarchy process method that is biased towards maximizing CCT with values of 0.7067 and 0.2933, respectively. Applying algorithm-A, the optimal allocation of the embedded TCSC for each particular line outage satisfying both system stability and maximum CCT is obtained as presented in Table 1. It could be seen from the results that it is required to insert TCSCs at 11 locations with different size to keep system stability at maximum CCT. The TCSCs are always capacitive and reduce the reactance of lines where they are located. Results of algorithm-A are considered as primary data for running sub-algorithm-B1. Accordingly, the sets based on location frequency are clustered and the equivalent set for each clus-

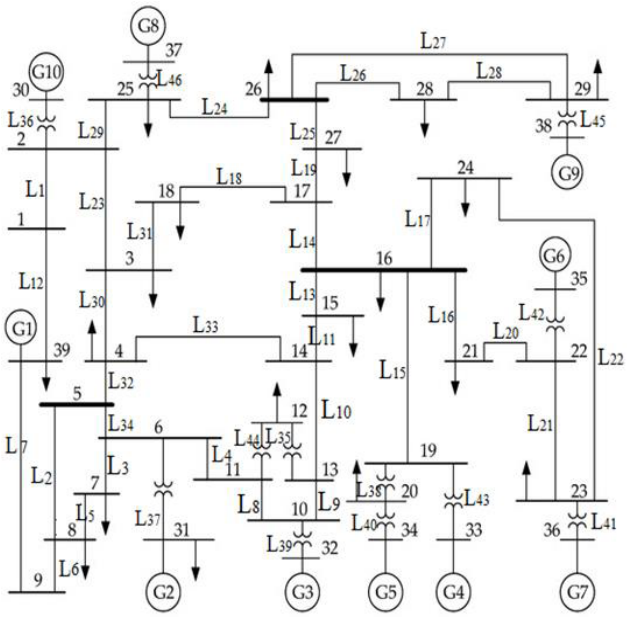

FIGURE 6. 39-bus ten machines New England test system with line numbers.

TABLE 1. Optimal allocation of TCSC for each faulted line.

Fault-Line, L #	Fault-line (From-To)	Optimal Location of TCSC			Compensation Degree (%)	Optimal size (p.u.)	Fault-Line, L #	Fault-line (From-To)	Optimal Location of TCSC			Compensation Degree (%)	Optimal size (p.u.)
		line No.	From Bus	To Bus					line No.	From Bus	To Bus		
1	2-1	30	3	4	-80	-0.017	24	26-25	4	11	6	-80	-0.006
2	5-8	30	3	4	-25.22	-0.005	25	27-26	4	11	6	-20.7	-0.001
3	6-7	30	3	4	-67.18	-0.014	26	28-26	4	11	6	-80	-0.006
4	11-6	11	15	14	-80	-0.010	27	29-26	4	11	6	-80	-0.006
5	7-8	23	2	3	-10	-0.001	28	29-28	30	3	4	-80	-0.017
6	8-9	10	13	14	-80	-0.008	29	2-25	11	15	14	-11.3	-0.002
7	39-9	31	18	3	-17.48	-0.002	30	3-4	11	15	14	-74	-0.016
8	10-11	11	15	14	-27.97	-0.006	31	18-3	4	11	6	-20.6	-0.001
9	10-13	11	15	14	-10	-0.002	32	4-5	11	15	14	-15	-0.003
10	13-14	14	16	17	-10	-0.001	33	14-4	11	15	14	-68.5	-0.015
11	15-14	13	39	9	-14	-0.001	34	6-5	14	16	17	-80	-0.007
12	1-39	14	16	17	-80	-0.007	35	13-12	11	15	14	-10	-0.002
13	15-16	14	16	17	-17.08	-0.001	36	2-30	10	13	14	-10	-0.001
14	16-17	33	14	4	-44.67	-0.005	37	6-31	14	16	17	-23.8	-0.002
15	16-19	4	11	6	-80	-0.004	38	19-20	4	11	6	-20	-0.001
16	21-16	12	1	39	-80	-0.014	39	10-32	31	18	3	-80	-0.011
17	24-16	33	14	4	-10	-0.001	40	20-34	14	16	17	-28.5	-0.002
18	17-18	30	3	4	-80	-0.017	41	23-36	18	17	18	-10	-0.001
19	17-27	4	11	6	-10	-0.001	42	22-35	30	3	4	-10	-0.002
20	22-21	33	14	4	-80	-0.010	43	19-33	4	11	6	-10	-0.001
21	23-22	33	14	4	-42.21	-0.005	44	11-12	11	15	14	-10	-0.002
22	24-23	4	11	6	-10	-0.001	45	29-38	30	3	4	-80	-0.017
23	2-3	33	14	4	-80	-0.010	46	25-37	30	3	4	-80	-0.017

ter, $G_{eq,i,}$ is deduced to define its cluster-TCSC as in the following:

$$G_1 = \{(\ell_1, -0.004), (\ell_1, -0.001), (\ell_1, -0.001), (\ell_1, -0.006), (\ell_1, -0.001), (\ell_1, -0.006), (\ell_1, -0.006), (\ell_1, -0.001), (\ell_1, -0.001), (\ell_1, -0.002)\}, \text{and}$$

$$G_{eq,1} = (\ell 1, -0.006), \ell_1 = L_4, k_1 = 10.$$

$$G_2 = \{(\ell_2, -0.01), (\ell_2, -0.006), (\ell_2, -0.002), (\ell_2, -0.002), (\ell_2, -0.016), (\ell_2, -0.003), (\ell_2, -0.015), (\ell_2, -0.002)(\ell_2, -0.002)\}, \text{and}$$

$$G_{eq,2} = (\ell_2, -0.016), \ell_2 = L_{11}, k_2 = 9.$$

$$G_3 = \{(\ell_3, -0.017), (\ell_3, -0.005), (\ell_3, -0.014), (\ell_3, -0, 017), (\ell_3, -0.017), (\ell_3, -0.002), (\ell_3, -0.017), (\ell_3, -0.017)\}, \text{and}$$

$$G_{eq,3} = (\ell_3, -0.017), \ell_3 = L_{30}, k_3 = 8.$$

$$G_4 = \{(\ell_4, -0.001), (\ell_4, -0.007), (\ell_4, -0.001), (\ell_4, -0.007), (\ell_4, 0.002), (\ell_4, -0.002)\}, \text{and}$$

$$G_{eq,4} = (\ell_4, -0.007), \ell_4 = L_{14}, k_4 = 6.$$

$$G_5 = \{(\ell_5, -0.001), (\ell_5 - 0.010), (\ell_5 - 0.010), (\ell_5 - 0.005), (\ell_5, -0.005)\}, \text{and}$$

$$G_{eq,5} = (\ell_5, -0.010), \ell_5 = L_{33}, k_5 = 5.$$

$$G_6 = \{(\ell_6, -0.002), (\ell_6, -0.011)\}, \text{and}$$

$$G_{eq,6} = (\ell_6, -0.011), \ell_6 = L_{31}, k_6 = 2.$$

$$G_7 = \{(\ell_7, -0.008), (\ell_7, -0.001)\}, \text{and}$$

$$G_{eq,7} = (\ell_7, -0.008), \ell_7 = L_{10,}k_7 = 2.$$

$$G_8 = \{(\ell_8, -0.001)\}, \text{and}$$

$$G_{eq,8} = (\ell_8, -0.001), \ell_8 = L_{13}, k_8 = 1$$

$$G_9 = \{(\ell_9, -0.002)\}, \text{and}$$

$$G_{eq,9} = (\ell_9, -0.002), \ell_9 = L_{18}, k_9 = 1$$

$$G_{10} = \{(\ell_{10}, -0.001)\}, \text{and}$$

$$G_{eq,10} = (\ell_{10}, -0.001), \ell_{10} = L_{23}, k_{10} = 1$$

$$G_{11} = \{(\ell_{11}, -0.014)\}, \text{and}$$

$$G_{eq,11} = (\ell_{11}, -0.014), \ell_{11} = L_{12}, k_{11} = 1.$$

Starting with the cluster-TCSC of the first cluster (G_1), as defined by (14), to be embedded into the power system, CT is applied to assess the system stability for all fault locations excluding those incorporated in this cluster, that is, for a number of fault locations, $N_F = 36$. The stability will be checked when inserting cluster-TCSCs one by one, i.e., in the order of L_4, L_{11}, L_{30}, L_{14}, L_{33}, L_{31}, L_{10}, L_{13}, L_{18}, L_{23}, and L_{12}. In each time, the number of fault locations, being tested, is recalculated according to (15). The results show that to cope with all probable line outage contingencies, BLN = 4 at locations L_4, L_{11}, L_{30}, and L_{14} with the size of -0.006, -0.016, -0.017, and -0.007 per unit, respectively. This means that use of the first four cluster-TCSCs defined by ($G_{eq,1}$ – $G_{eq,4}$) is sufficient to maintain system stability for all probable contingencies. Then, from the allocated TCSCs, the selection of those satisfying the BHV of CCT and maintaining system stability is obtained by applying the sub-algorithm-B2 as given in Table 2. It is found that for fault-lines in Table 1 at which the TCSC location belongs to the first four clusters (G_1-G_4) have the same TCSC location as that in Table 2, whereas the rest of cases (belonging to clusters G_5-G_{11}) have different locations.

TABLE 2. TCSCs for BHV of CCT for line outage.

Fault-Line, L #r	Fault-line (From-To)	Location of cluster-TCSC	Fault-Line, L #	Fault-line (From-To)	Location of cluster-TCSC
1	2-1	L_{30}	24	26-25	L_4
2	5-8	L_{30}	25	27-26	L_4
3	6-7	L_{30}	26	28-26	L_4
4	11-6	L_{11}	27	29-26	L_4
5	7-8	L_{14}	28	29-28	L_{30}
6	8-9	L_{30}	29	2-25	L_{11}
7	39-9	L_{30}	30	3-4	L_{11}
8	10-11	L_{11}	31	18-3	L_4
9	10-13	L_{11}	32	4-5	L_{11}
10	13-14	L_{14}	33	14-4	L_{11}
11	15-14	L_{14}	34	6-5	L_{14}
12	1-39	L_{14}	35	13-12	L_{11}
13	15-16	L_{14}	36	2-30	L_{14}
14	16-17	L_4	37	6-31	L_{14}
15	16-19	L_4	38	19-20	L_4
16	21-16	L_{14}	39	10-32	L_{14}
17	24-16	L_{14}	40	20-34	L_{14}
18	17-18	L_{30}	41	23-36	L_{14}
19	17-27	L_4	42	22-35	L_{30}
20	22-21	L_4	43	19-33	L_4
21	23-22	L_4	44	11-12	L_{11}
22	24-23	L_4	45	29-38	L_{30}
23	2-3	L_4	46	25-37	L_{30}

For instance, a three-phase fault occurs at the line, L #29, from bus #2 to #25, close to bus #25 is considered to numerically illustrate the process. The fault is cleared by tripping the faulted line. It is found that the system is unstable according

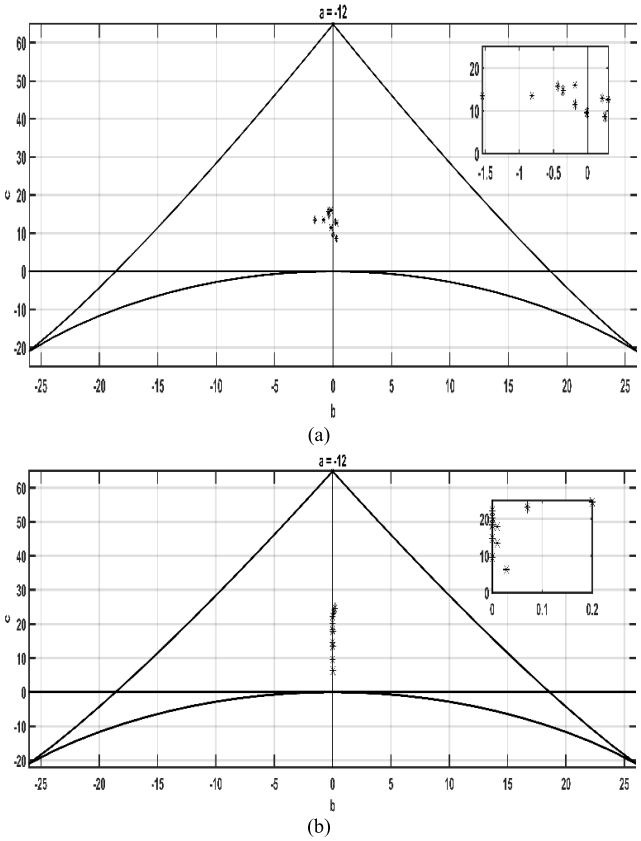

FIGURE 7. Location of operating points in bifurcation set. (a) Without TCSC, (b) With TCSC at location L_{11}. Fault at L #29.

to the location of the operating points in the bifurcation set as shown in Fig. 7a. As the results obtained from applying the primary part of the proposed algorithm (algorithm-A) and given in Table 1, the system needs to insert the TCSC located at L_{11} to satisfy both stability and maximum CCT. Then, by using the complementary part of the proposed algorithm (algorithm-B), it is found that the same TCSC is selected among 4 sets of TCSC (BLN = 4) to be inserted in the system as in Table 2 and the operating points are located inside the stable region, Fig. 7b. In addition, the BHV of CCT compared with the maximum CCT obtained by PSO technique is almost the same or with very slight increase/decrease for some generators as given in Table 3. CT evaluates the CCT for each generating unit, and so, the least value of CCT is taken as the influential CCT value.

Applying the same procedure to the system when a fault occurs at line, L #14, it is seen that the TCSC required to satisfy system stability and maximum CCT is located at L_{33} as given in Table 1, whereas satisfying system stability and BHV of CCT entails the TCSC to be located at L_4, Table 2. The change of TCSC allocation is due to that the location L_{33} belongs to cluster G5, i.e., it is out of the first four clusters (G1, . . ., G4) and thus, the BHVs of CCT differ from the corresponding maximum values as in Table 4. However, this change does not affect system stability satisfaction and

TABLE 3. Values of CCTs (s) for uncompensated and compensated system at the line, L #29.

Generator No.	Gen_1	Gen_2	Gen_3	Gen_4	Gen_5	Gen_6	Gen_7	Gen_8	Gen_9	Gen_{10}
CCT uncompensated system	0.3141	0.3135	0.3243	0.3865	0.281	0.329	0.241	0.59	0.9	0.316
Maximum CCT	0.3730	0.3997	0.3881	0.4268	0.344	0.3296	0.298	0.886	1.475	0.435
BHV of CCT	0.3727	0.392	0.388	0.4257	0.328	0.312	0.287	0.734	1.423	0.440

TABLE 4. Values of CCTs (s) for uncompensated and compensated system at the line, L #14.

Generator No.	Gen_1	Gen_2	Gen_3	Gen_4	Gen_5	Gen_6	Gen_7	Gen_8	Gen_9	Gen_{10}
CCT uncompensated system	0.3462	0.3239	0.3571	0.3719	0.2583	0.3778	0.301	0.729	0.890	0.287
Maximum CCT	0.3860	0.5635	0.4617	0.6054	0.3751	0.328	0.422	0.902	1.474	0.961
BHV of CCT	0.3643	0.4011	0.4142	0.4354	0.338	0.381	0.310	0.901	1.449	0.587

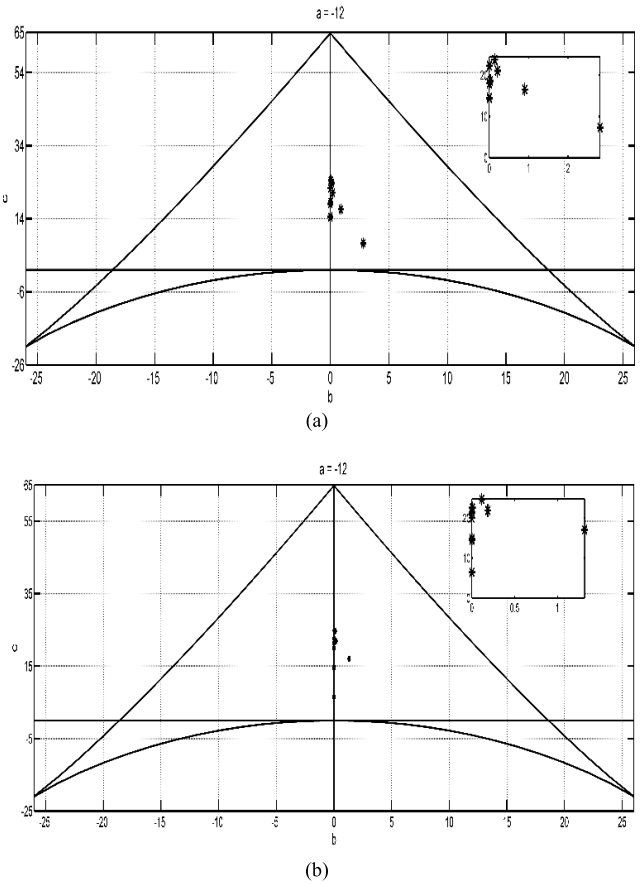

FIGURE 8. Location of operating points in bifurcation set with (a) TCSC of location L_{33} and (b) TCSC of location L_4. Fault at L #14.

increases the CCT of the uncompensated system generators, which is the main goal and has the major priority in all similar cases. Fig. 8 shows that all operating points are inside the stable region of the bifurcation set when applying the TCSC of locations L_{33} and L_{14}.

TDS is considered as the most validated method which can reflect all the dynamics of the power system under several disturbances. Therefore, the results obtained by the proposed algorithm are compared with those through TDS. For the same fault location (L #29) and the corresponding TCSC location (L_{11}) as in the numerical example, TDS is done by using PSAT MATLAB [45]. The fault occurred at 0 s and is cleared after 0.26 s by tripping the faulted line (L #29).

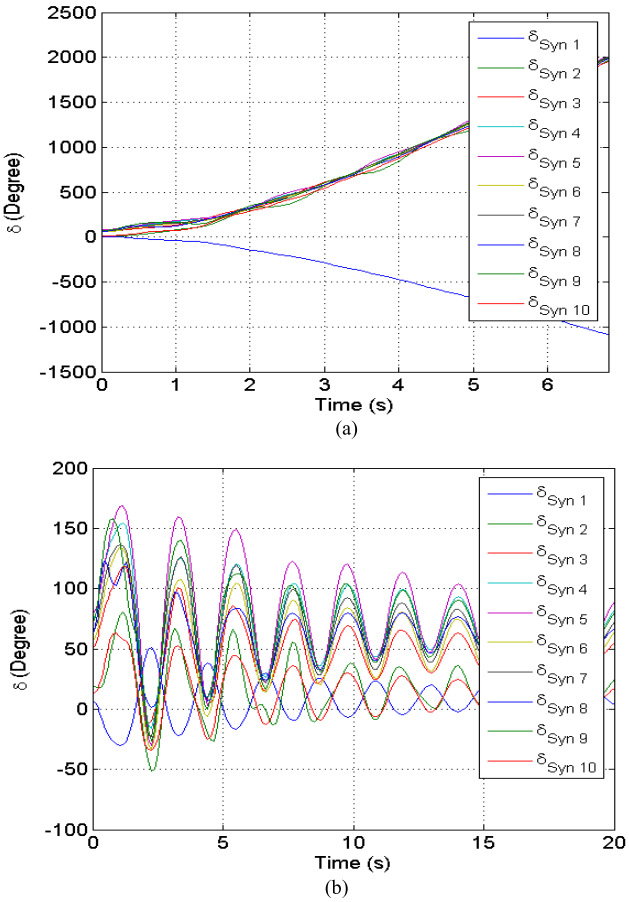

FIGURE 9. Power angle δ^o versus time in s for a fault at L #29, (a) uncompensated system and (b) compensated system.

Fig. 9 shows the curve of power angle δ^o versus time in s for the generating units in both compensated and uncompensated system. It could be seen from Fig. 9a that the uncompensated system is unstable. By inserting the TCSC in line L_{11}

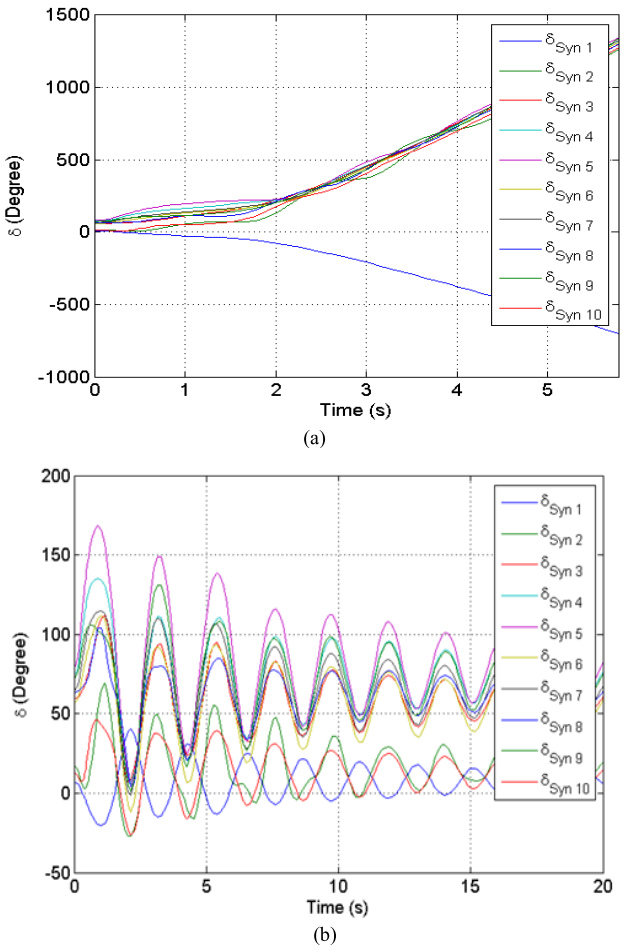

FIGURE 10. Power angle δ^{o} versus time in s for a fault at L #14, (a) uncompensated system and (b) compensated system.

according to the algorithm's results, the system regains its stability as shown in Fig. 9b. Similarly, TDS is applied when the fault occurs at L #14. The fault occurred at 0 s and is cleared after 0.26 s by tripping the faulted line. Fig. 10 shows power angle δ^{o} versus time. The instability of uncompensated system is depicted in Fig. 10a. With compensating the system by connecting the TCSC to line L_4 according to the algorithm's results, the system becomes stable, Fig. 10b. System congestion is also considered in order to evaluate the proposed algorithm at a different kind of disturbance. The congestion is considered as a sudden increase in the largest load connected to bus # 39 by 60% of its rated value. Fig.11 shows the location of operating points in bifurcation set with using the four TCSC devices as resulted from the algorithm. As seen in this figure, all the operating points are located in the stability region as an indication of system stability. The δ^{o}-time curve of Fig. 12 shows the stability state of the system which confirms the result of the proposed algorithm. Furthermore, as given in Table 5, the values of CCT obtained by CT are very close to those computed by TDS method.

TABLE 5. CCT comparison between TDS and the proposed algorithm.

	Uncompensated system		Compensated system	
Fault location	TDS (s)	Algorithm (s)	TDS (s)	Algorithm (s)
L#29	0.236	0.241	0.263	0.287
L#14	0.256	0.258	0.275	0.31

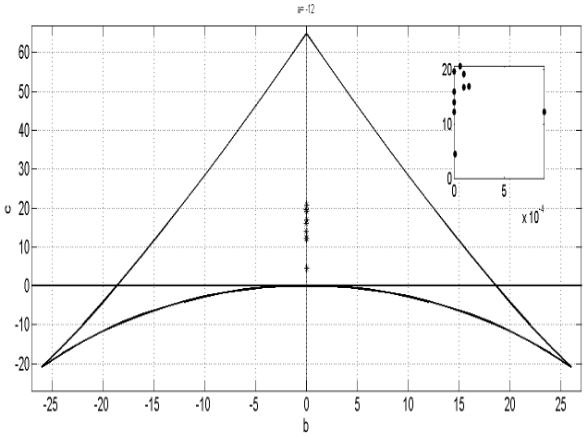

FIGURE 11. Location of operating points in bifurcation set with TCSCs located on (L4, L11, L30, and L14) for 60% increase of load at bus #39.

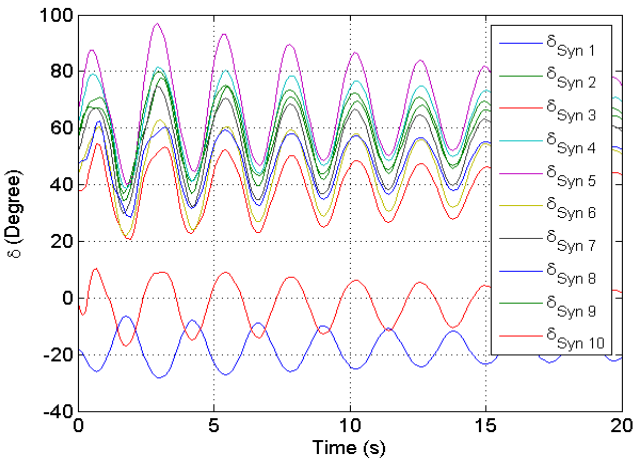

FIGURE 12. Power angle delta in degree versus time in s for 60% increase of load at bus #39.

VII. CONCLUSIONS

A novel algorithm is presented in this paper with a view to improving the transient stability in an optimal way. The algorithm is based on a proposed clustering technique combined with CT and MOPSO in order to define the BLN and allocation of TCSC in a technical and an economical manner. Visualizing the stability state of the power system by monitoring the location of the operating points in the swallowtail bifurcation set is also an additional gain. Remarkable observations have been achieved such as the significant reduction

in the number of necessary and sufficient TCSCs to enhance system stability (from 11 to 4 devices, i.e., 64% reduction). The allocation of TCSC devices is appropriately identified so that it has a significant effect on the stability of the test system. Therefore, stability margin has been increased by rising the values of CCTs for each generator by almost 15% to operate more securely and enhance the location of operating points in the CT's stability region. The superiority of the proposed algorithm has been shown in the case of system congestion where the allocation of the selected TCSC devices enables the system to retain stability in spite of congestion by 60% increase in the largest load. The effectiveness of the proposed algorithm has been demonstrated by computational studies on 39-bus ten-machine New England power system. Comparing the results of the proposed algorithm with those through TDS provides the proposed algorithm an extra dimension for confirmation.

Appendix

As reported in [13], a generator connected to an integrated power system can generally configure as shown in Fig. 13. The electrical output power P_{ei} of generator G_i is

$$P_{ei} = \mathrm{Re}[I_i E_i^*] \tag{A.1}$$

$$I_i = (E_q - E_i)/jX_q \tag{A.2}$$

$$E_i = (-1/Y_{ij}) \sum_{\substack{J=1 \\ \neq i}}^{N} Y_{ij} E_j \tag{A.3}$$

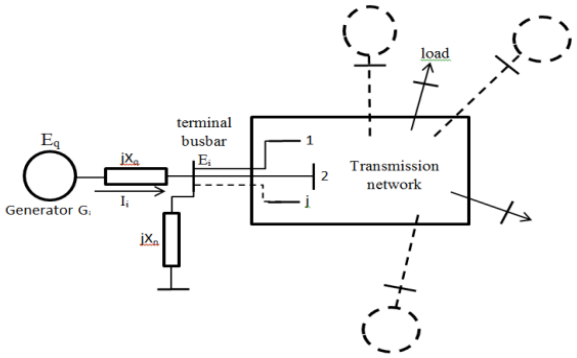

FIGURE 13. Representation of generator G_i connected to an integrated power system.

where,
I_i = generator current following into terminal bus bar
E_i = terminal bus bar voltage
N = number of the network bus bars plus the internal machine bus bars.
Y_{ij} = off-diagonal element of the admittance matrix.
E_q = machine internal voltage source behind quadrature-reactance. therefore,

$$E_i = \frac{1}{\left(\frac{1}{jX_n}\right) + \sum_{\substack{j=1 \\ \neq i}}^{N} \left(\frac{1}{jX_{ij}}\right)} \sum_{\substack{j=1 \\ \neq i}}^{N} \left(\frac{E_j}{jX_{ij}}\right) \tag{A.4}$$

Assuming e and f, are the real and imaginary components of the voltage E, respectively. Substituting (A.4) into (A.1), we get:

$$\mathrm{Pei} = \mathrm{Re}\left[\frac{e_q + jf_q}{jX_q}\left(\frac{1}{\frac{1}{jX_n} + \sum_{\substack{j=1 \\ \neq i}}^{N}\left(\frac{1}{jX_{ij}}\right)} \sum_{\substack{j=1 \\ \neq 1}}^{N} \frac{e_j + jf_j}{jX_{ij}}\right) - \frac{1}{jX_q}\left(e_i^2 + f_i^2\right)\right] \tag{A.5}$$

i.e.,

$$\mathrm{Pe} = \frac{\frac{1}{X_q}}{\frac{1}{X_n} + \sum_{\substack{j=1 \\ \neq i}}^{N} \frac{1}{X_{ij}}} \times \left[f_{qi} \sum_{\substack{j=1 \\ \neq i}}^{N}\left(\frac{e_j}{X_{ij}}\right) - e_{qi} \sum_{\substack{j=1 \\ \neq i}}^{N}\left(\frac{f_j}{X_{ij}}\right)\right] \tag{A.6}$$

Let

$$\psi = \left(\frac{1}{X_q}\right) / \left(\frac{1}{X_n} + \sum_{\substack{j=1 \\ \neq i}}^{N} \frac{1}{X_{ij}}\right) \tag{A.7}$$

$$\sigma_1 = \sum_{\substack{j=1 \\ \neq i}}^{N}\left(\frac{e_j}{X_{ij}}\right) \tag{A.8}$$

$$\sigma_2 = \sum_{\substack{j=1 \\ \neq i}}^{N}\left(\frac{f_j}{X_{ij}}\right) \tag{A.9}$$

$$A_1 = \psi E_q \sigma_1 \tag{A.10}$$

$$A_2 = \psi E_q \sigma_2 \tag{A.11}$$

Then, (A.6) becomes

$$P_{ei} = A_1 \sin\delta_i - A_2 \cos\delta_i \tag{A.12}$$

where
$\delta_i = tan^{-1}\left(\frac{f_q}{e_q}\right)$ = machine power angle referred to the common reference axes of the system.

The equation of motion of generator G_i with respect to the common reference axes of the network is

$$M_I \ddot{\delta_i} = P_{in} - P_{ei} \tag{A.13}$$

where,
M_i = inertia constant of machine i.
P_{in} = input mechanical power. Multiplying (A.13) by $d\delta/dt$ and integrating, we obtain

$$(d\delta/dt)^2 = \int_{\delta_0}^{\delta_m} (P_{in} - P_{ei})\, d\delta \tag{A.14}$$

δ_0, δ_m are the minimum and maximum angles of oscillation, respectively. The machine will again retain synchronism after a disturbance when $d\delta/dt = 0$, i.e., the RHS of (A.14) must equal zero. In other words, the machine is stable if the kinetic energy generated during the fault is less than, or equal (totally converted) to, the potential energy during the post

fault period. The equality of both energies takes place in the critical clearing case, i.e.,

$$F = F_{ke} + F_{pe} = 0 \tag{A.15}$$

By catastrophe theory, the equilibrium surface U of a smooth function F is given by

$$U = \nabla F_c(x) = F = F_{ke} + F_{pe} = 0 \tag{A.16}$$

and the singularity set S which is defined as the set of steady-state stability limits is obtained by

$$\nabla^2 F_c(x) = 0 \tag{A.17}$$

The transient kinetic energy can be evaluated by the amount of output power reduction during the fault. Therefore, it is expressed by

$$F_{ke} = \int_{\delta_0}^{\delta_c} (P_{in} - P_{ei})\, d\delta \tag{A.18}$$

The potential energy after the fault is

$$F_{pe} = \int_{\delta_c}^{\delta_m} (P_{in} - P_{ei})\, d\delta \tag{A.19}$$

From (A.16), (A.18), and (A.19), the following relation is obtained:

$$(A_{1D} + A_{1A}) \cos\delta_c + (A_{2A} - A_{2D}) \sin\delta_c + K = 0 \tag{A.20}$$

where,
A_{iD} = the coefficient A_i, (i = 1,2) during the fault
A_{iA} = the coefficient A_i, (i = 1,2) after fault
δc = critical clearing angle
K = constant = K_2- K_1

$$K_1 = A_{1D} \cos\delta_0 - A_{2D} \sin\delta_0 - P_{in}\delta_0 \tag{A.21}$$
$$K_2 = -(A_{1A} \cos\delta_m + A_{2A} \sin\delta_m + P_{in}\delta_m) \tag{A.22}$$

Replacing sin and cos by their expansion, and assuming = x, (A.20) can be rewritten as:

$$(A_{1D} + A_{1A}) \left(1 - \frac{x^2}{2!} + \frac{x^4}{4!} \ldots\ldots\right) + (A_{2A} - A_{2D}) \left(x - \frac{x^3}{3!} + \frac{x^5}{5!} \ldots\ldots\right) + K = 0 \tag{A.23}$$

If the series expansion in (A.23) is trunked up to fourth order terms, it gives

$$B_4 x^4 + B_3 x^3 + B_2 x^2 + B_1 x + B_0 = 0 \tag{A.24}$$
$$B_0 = A_{1D} + A_{1A} + K \tag{A.25}$$
$$B_1 = A_{2A} - A_{2D} \tag{A.26}$$
$$B_2 = -(A_{1A} + A_{1D})/2 \tag{A.27}$$
$$B_3 = (A_{2D} - A_{2A})/6 \tag{A.28}$$
$$B_4 = (A_{1D} + A_{1A})/24 \tag{A.29}$$

Equation (A.24) is four-determinate and closely equivalent to (A.20). The cubic term can be eliminated by taking x = y-α and $\alpha = B_3/4B_4$ to get the form

$$y^4 + ay^2 + by + c = 0 \tag{A.30}$$

where,

$$a = (6B_4\alpha^2 - 3B_3\alpha + B_2)/B_4 \tag{A.31}$$
$$b = (3B_3\alpha^2 - 2B_2\alpha + B_1)/B_4 - 4\alpha^3 \tag{A.32}$$
$$c = \alpha^4 + (B_0 - B_1\alpha + B_2\alpha^2 - B_3\alpha^3) \tag{A.33}$$

The smallest positive real root of the swallowtail equation, y, satisfying the relation $\delta\, o < y - \alpha < \delta m$ gives the critical clearing angle δ_c for the stable machines in the system. They can be represented by operating points which lie inside the bifurcation set B. CCT can be calculated by using Taylor approximations for δ_c and its derivative $\delta_c^{\cdot}$, which gives a good result for the first swing analysis, as follows:

$$\delta_c = w_c = \gamma t_c \tag{A.34}$$

where,

$$\gamma \triangleq \text{machine acceleration at the istant of fault occurance} = (1/M)\,[P_{in} - P_e(t_{o+})] \tag{A.35}$$

and

$$\delta_c = \delta_0 + \frac{1}{2}\gamma t_c^2 \tag{A.36}$$

then,

$$CCT = \sqrt{\frac{2}{\gamma}(\delta_c - \delta_0)} = \sqrt{\frac{2M(\delta_c - \delta_0)}{(P_{in} - P_e(t_{o+}))}} \tag{A.37}$$

REFERENCES

[1] P. Kundur *et al.*, "Definition and classification of power system stability," *IEEE Trans. Power Syst.*, vol. 19, no. 3, pp. 1387–1401, Aug. 2004, doi: 10.1109/TPWRS.2004.825981.

[2] N. Yorino, A. Priyadi, H. Kakui, and M. Takeshita, "A new method for obtaining critical clearing time for transient stability," *IEEE Trans. Power Syst.*, vol. 25, no. 3, pp. 1620–1626, Aug. 2010, doi: 10.1109/TPWRS.200-9.2040003.

[3] S. Sowmya and K. Anuradha, "A novel approach to transient stability using stochastic energy functions suitable for power system risk assessment," *Int. J. Eng. Sci.*, vol. 3, no. 1, pp. 40–47, 2014.

[4] H.-F. Zhou, F. Tang, J. Jia, and X.-L. Ye, "The transient stability analysis based on WAMS and online admittance parameter identification," in *Proc. IEEE PowerTech Eindhoven*, Jun. 2015, pp. 1–6, doi. 10.1109/PTC.2015.7232544.

[5] I. B. Sulistiawati, A. Priyadi, O. A. Qudsi, A. Soeprijanto, and N. Yorino, "Critical Clearing Time prediction within various loads for transient stability assessment by means of the Extreme Learning Machine method," *Int. J. Elect. Power Energy Syst.*, vol. 77, pp. 345–352, May 2016, doi: 10.1016/j.ijepes.2015.11.034.

[6] Y. Lin, "Explaining critical clearing time with the rules extracted from a multilayer perceptron artificial neural network," *Int. J. Elect. Power Energy Syst.*, vol. 32, no. 8, pp. 873–878, Oct. 2010, doi: 10.1016/j.ijepes.2010.01.026.

[7] Y. Kato, K. Yoda, T. Ohtaka, and S. Iwamoto, "Use of critical clearing time for transient stability preventive control," *IFAC Proc. vol.*, vol. 36, no. 20, pp. 1127–1132, Sep. 2003, doi: 10.1016/S1474-6670(17)34626-8.

[8] A. M. Mihirig and M. D. Wvong, "Catastrophe theory applied to transient stability assessment of power systems," *IEE Proc. C—Gener. Transm. Distrib.*, vol. 133, no. 6, pp. 314–318, Sep. 1986, doi: 10.1049/ip-c:19860046.
[9] R. Parsi-Feraidoonian, "Application of catastrophe theory to transient stability analysis of power systems," M.S. thesis, Dept. Elect. Eng., Univ. British Columbia, Vancouver, BC, Canada, 1990.
[10] A. A. Sallam and J. L. Dineley, "Catastrophe theory as a tool for determining synchronous power system dynamic stability," *IEEE Trans. Power App. Syst.*, vol. PAS-102, no. 3, p. 622–630, Mar. 1983, doi. 10.1109/TPAS.1983.317-983.
[11] A. A. Sallam and J. L. Dineley, "Catastrophe theory applied to power system steady state stability—A comparison with the energy—Balanced approach," in *Proc. 8th Power Syst. Comp. Conf.*, Helsinki, Finland, Aug. 1984, pp. 915–922.
[12] A. M. Mihirig and M. D. Wvong, "Transient stability analysis of multimachine power system by catastrophe theory," *IEE Proc. C—Gener., Transm. Distrib.*, vol. 136, no. 4, pp. 254–258, Jul. 1989, doi: 10.1049/ipc.1989.033.
[13] A. A. Sallam, "Power systems transient stability assessment using catastrophe theory," *IEE Proc. C—Gener., Transm. Distrib.*, vol. 136, no. 2, pp. 108–114, Mar. 1989, doi: 10.1049/ip-c.1989.0016.
[14] S. A. Soliman and A. H. Mantawy, "Mathematical optimization techniques," in *Modern Optimization Techniques with Applications in Electric Power Systems*, 1st ed. New York, NY, USA: Springer, 2012, pp. 23–81, ch. 2. [Online]. Available: http://www.springer.com/gp/book/978-146141751-4
[15] Q. Lin, J. Li, Z. Du, J. Chen, and Z. Ming, "A novel multi-objective particle swarm optimization with multiple search strategies," *Euro. J. Oper. Res.*, vol. 247, no. 3, pp. 732–744, Dec. 2015, doi: 10.1016/j.ejor.2015.06.071.
[16] R. Moslemi, H. A. Shayanfar, and L. Wng, "Multi-objective particle swarm optimization for transient secure congestion management," in *Proc. Int. Conf. Environ. Elect. Eng. (EEEIC)*, May 2012, pp. 590–594.
[17] A. D. Falehi and A. Mosallanejad, "Dynamic stability enhancement of interconnected multi-source power systems using hierarchical ANFIS controller-TCSC based on multi-objective PSO," *Frontiers Inform. Technol. Electron. Eng.*, vol. 18, no. 3, pp. 394–409, Mar. 2017.
[18] M. Gitizadeh and S. Ghavidel, "Improving transient stability with multi-objective allocation and parameter setting of SVC in a multi-machine power system," *IETE J. Res.*, vol. 60, no. 1, pp. 33–41, Jun. 2014, doi: doi.org/10.1080/037720 63.2014.890814.
[19] M. S. Rawat and S. Vadhera, "Comparison of FACTS devices for transient stability enhancement of multi machine power system," in *Proc. IEEE Int. Conf. Microelectron. Comp. Commun.* , Jun. 2016, pp. 1–5.
[20] A. A. Sallam and P. Om Malik, "Compensation devices," in *Power System Stability: Modelling, Analysis, and Control*, 1st ed. London, U.K.: IET Press, 2015, pp. 379–393, ch. 14. [Online]. Available: https://www.theiet.org/resource-s/books/powen/powersys.cfm
[21] A. Jain, L. K. Yadav, A. Omer, and S. Bhullar, "Analysis of effectiveness of SSSC in transmission network using PI controlled technique," *Energy Procedia*, vol. 117, pp. 699–707, Jun. 2017, doi. 10.1016/j.egypro.2017.05.184.
[22] A. Rashad, S. Kamel, and F. Jurado, "Stability improvement of power systems connected with developed wind farms using SSSC controller," *Ain Shams Eng. J.*, to be published, doi: 10.1016/j.asej.2017.03.015.
[23] M. Mandala and C. P. Gupta, "Optimal placement of TCSC for congestion management using modified particle swarm optimization," *Int. J. Comput. Appl.*, vol. 88, no. 11, pp. 34–40, Feb. 2014.
[24] S. Raj and B. Bhattacharyya, "Optimal placement of TCSC and SVC for reactive power planning using Whale optimization algorithm," *Swarm Evol. Comput.*, to be published, doi: 10.1016/j.s-wevo.2017.12.0-08.
[25] A. K. Mohanty and A. K. Barik, "Power system stability improvement using FACTS devices," *Int. J. Modern Eng. Res.*, vol. 1, no. 2, pp. 666–672, 2011. [Online]. Available: http://www.ijmer.com/papers/Full-Issue/Vol.1_issue2.pdf
[26] V. G. Mathad, B. F. Ronad, and S. H. Jangamshetti, "Review on comparison of FACTS controllers for power system stability enhancement," *Int. J. Sci. Res. Publication*, vol. 3, no. 3, pp. 2250-2315, Mar. 2013.
[27] M. Dogan, S. Tosun, A. Ozturk, and M. K. Dosoglu, "Investigation of TCSC and SSSC controller effects on the power system," in *Proc. 7th Int. Con. Elec. Electron. Eng.*, Bursa, Turkey, Dec. 2011, pp. 1–4.
[28] M. Nandi, C. K. Shiva, and V. Mukherjee, "TCSC based automatic generation control of deregulated power system using quasi-oppositional harmony search algorithm," *Eng. Sci. Technol. Int. J.*, vol. 20, pp. 1380–1395, Aug. 2017, doi: 10.1016/j.jestc-h.2016.08.021.
[29] J. Morsali, K. Zare, and M. T. Hagh, "Applying fractional order PID to design TCSC-based damping controller in coordination with automatic generation control of interconnected multi-source power system," *Eng. Sci. Technol. Int. J.*, vol. 20, pp. 1–17, Feb. 2017, doi: 10.1016/j.jestch.20-16.06.002.
[30] M. Nandi, C. K. Shiva, and V. Mukherjee, "Frequency stabilization of multi-area multi-source interconnected power system using TCSC and SMES mechanism," *J. Energy Stor.*, vol. 14, pp. 348–362, Dec. 2017.
[31] J. Morsali, K. Zare, and M. T. Hagh, "Performance comparison of TCSC with TCPS and SSSC controllers in AGC of realistic interconnected multi-source power system," *Ain Shams Eng. J.*, vol. 7, no. 1, pp. 143–158, Mar. 2016, doi: 10.1016/j.asej.2015.11.012.
[32] W. S. Sakr, R. A. El-Sehiemy, and A. M. Azmy, "Optimal allocation of TCSCs by adaptive DE algorithm," *IET Gener., Transm. Distrib.*, vol. 10, no. 15, pp. 3854–3855, Nov. 2016, doi: 10.1049/iet-gtd.2016.0362.
[33] M. Bakhshi, M. H. Holakooie, and A. Rabiee, "Fuzzy based damping controller for TCSC using local measurements to enhance transient stability of power systems," *Elec. Power Energy Syst.*, vol. 85, pp. 12–21, Feb. 2017, doi: 10.1016/j.ijepes.2016.06.014.
[34] A. Haldera, N. Palb, and D. Mondalc, "Transient stability analysis of a multimachine power system with TCSC controller—A zero dynamic design approach," *Int. J. Elect. Power Energy Syst.*, vol. 97, pp. 51–71, Apr. 2018, doi: 10.1016/j.ijepes.2017.-10.030.
[35] M. Hanyi and D. Chen, "Multi-objective coordinated design of TCSC and SVC for improving transient stability," in *Proc. 5th Int. Conf. IEEE Instrum., Meas., Comput., Commun. Control*, Sep. 2015, pp. 246–250, doi: 10.1109/IMCCC.2015.59.
[36] R. Glimore, "The crowbar principle," in *Catastrophe Theory for Scientists and Engineers*, 1st ed. New York, NY, USA: Dover, 1993, ch. 5. pp. 51–93 [Online]. Available: http://www.bookd-epository.com/Catastroph-eTheory-forSc-ientists-Engineers-Robert-Gilmore/9780-486675398
[37] G. I. Rashed, H. I. Shaheen, and S. J. Cheng, "Optimal location and parameter settings of multiple TCSCs for increasing power system loadability based on GA and PSO techniques," in *Proc. 3rd Int. Con. Nat. Comput.*, Aug. 2007, pp. 335–344.
[38] P. M. Anderson and R. G. Farmer, "Subsynchronous resonance," in *Series Compensation of Power Systems*, 1st ed. California, CA, USA: PBLSH Inc., 1996, ch 6, pp. 229–286. [Online].Available: http://trove.nla.gov.au/work/1493-1186?q&versionId=175845 26.
[39] P. YengYin, "Movement strategy for multi-objective particle swarm optimization," in *Modeling, Analysis, and Applications in Metaheuristic Computing: Advancements and Trends*, 1st ed. Hershey, PA, USA: IGI Global, 2012, ch. 8, pp. 109–130. [Online]. Available: https://dl.acm.org/citation.cf-m?id=23413-52
[40] S. Kaddani, D. Vanderpooten, J.-M. Vanpeperstraete, and H. Aissi, "Weighted sum model with partial preference information: Application to multi-objective optimization," *Euro. J. Oper. Res.*, vol. 260, pp. 1–29, Jan. 2017, doi: 10.1016/j.ejor.2017.01.003.
[41] A. Datta, D. Saha, A. Ray, and P. Das, "Evaluation of anti-islanding techniques for renewable energy powered distributed generators using analytic network process," *IET Renew. Power Generat.*, vol. 10, no. 9, pp. 1245–1254, Oct. 2016.
[42] J. Rezaein, "Best-worst multi-criteria decision-making method," *Omega*, vol. 53, pp. 49–57, Jun. 2015.
[43] O. Cheikhrouhou, A. Koubâa, and A. Zaard, "Analytical hierarchy process based multi-objective multiple traveling salesman problem," in *Proc. IEEE Int. Conf. Auton. Robot Syst. Compet.*, Brigance, Portugal, May 2016, pp. 130–136.
[44] K. R. Padiyar, *Power System Dynamics: Stability and Control*, 2nd ed. Hyderabad, India: BS Pub, 2006. [Online]. Available: http://www.abebooks.com/Power-Syste-m-Dynamics-Stability-Control-Padiyar/1267253960/bd
[45] M. Federico, L. Vanfretti, and J. C. Morataya, "An open source power system virtual laboratory: The PSAT case and experience," *IEEE Trans. Edu.*, vol. 51, no. 1, pp. 17–23, Feb. 2008.

MAI MAHMOUD ELADANY received the B.Sc. and M.Sc. degrees from the Faculty of Engineering, Port Said University, Egypt, in 2007 and 2012, respectively. She is currently an Assistant Teacher with the Department of Electrical Engineering, Faculty of Engineering, Port Said University. Her research interests include power system transient stability, smart grids, and renewable energy.

AZZA AHMED ELDESOUKY received the B.S. and M.S. degrees in electrical engineering from Suez Canal University in 1989 and 1995, respectively, and the Ph.D. degree from the University of Bath, U.K., in 2002. She is currently an Assistant Professor of electrical power engineering at Port Said University. Her research interests include power system operation and management, microgrid stability and control, smart grids, and distributed generation systems.

ABDELHAY AHMED SALLAM (M'68–SM'94–LSM'14) received the B.Sc., M.Sc., and Ph.D. degrees from the Faculty of Engineering, Cairo University, Egypt, in 1967, 1972, and 1976, respectively. From 1967 to 1979, he was with the Ministry of Industry. In 1980, he joined the Department of Electrical Engineering, Faculty of Engineering, Suez Canal University, then, Port Said University, Egypt, where he is currently a Professor (Emeritus).

From 1981 to 1983, he was a Visiting Member of Staff with the Department of Electrical and Electronic Engineering, Newcastle University, Newcastle upon Tyne, U.K. In 1997, he joined Canal Electricity Company as the Head of Technical Affairs Sector, where he spent four years. In 2006, 2007, 2009, 2012, and 2014, he was a Visiting Professor with the Department of Electrical and Computer Engineering, University of Calgary, Calgary, AB, Canada.

He has authored or co-authored over 100 papers in international journals and conferences. He is the author of two books *Electric Distribution Systems* (IEEE-John Wiley & Sons Press, 2011) and *Power System Stability: Modelling, Analysis and Control* (IET, 2015). His field of interest is mainly the power system analysis and planning.